

Video-based computer navigation in knee arthroscopy for patient specific ACL reconstruction

Carolina Raposo^{1,2} · João P. Barreto^{1,2} ·
Cristóvão Sousa² · Luis Ribeiro² · Rui
Melo² · João Pedro Oliveira³ · Pedro
Marques³ · Fernando Fonseca³ · David
Barrett⁴

Received: date / Accepted: date

Abstract

Purpose The Anterior Cruciate Ligament (ACL) tear is a common medical condition that is treated using arthroscopy by pulling a tissue graft through a tunnel opened with a drill. The correct anatomical position and orientation of this tunnel is crucial for knee stability, and drilling an adequate bone tunnel is the most technically challenging part of the procedure. This paper presents the first guidance system based solely on intra-operative video for guiding the drilling of the tunnel.

Methods Our solution uses small, easily recognizable visual markers that are attached to the bone and tools for estimating their relative pose. A recent registration algorithm is employed for aligning a pre-operative image of the patient's anatomy with a set of contours reconstructed by touching the bone surface with an instrumented tool.

Results Experimental validation using ex-vivo data shows that the method enables the accurate registration of the pre-operative model with the bone, providing useful information for guiding the surgeon during the medical procedure. Experiments also demonstrate that the guided drilling of the tunnel leads to errors as low as 2.5mm in the footprint and 1.8° in orientation, which compares favorably to other works in the field [6].

Conclusion The high accuracy and short time overhead evinced by the experimental validation combined with no additional incisions or capital equipment

The authors thank the Portuguese Science Foundation and COMPETE2020 program for generous funding through project VisArthro (ref.: PTDC/EEIAUT/3024/2014). This paper was also funded by the European Union's Horizon 2020 research and innovation programme under grant agreement No 766850.

¹ Institute of Systems and Robotics, University of Coimbra, Portugal · ² Perceive3D, Coimbra, Portugal · ³ Coimbra Hospital and University Centre, Faculty of Medicine, Coimbra, Portugal · ⁴ Bioengineering Science Research Group, School of Engineering Sciences, University of Southampton, UK

make this video-based Computer-Aided Arthroscopy (CAA) solution an appealing alternative to the existing approaches.

Keywords Computer-guidance, Visual tracking, 3D Registration, Arthroscopy

1 Introduction

Arthroscopy is a modality of orthopaedic surgery for treatment of damaged joints in which instruments and endoscopic camera (the arthroscope) are inserted into the articular cavity through small incisions (the surgical portals). Since arthroscopy largely preserves the integrity of the articulation, it is beneficial to the patient in terms of reduction of trauma, risk of infection and recovery time [28]. However, arthroscopic approaches are more difficult to execute than the open surgery alternatives because of the indirect visualization and limited manoeuvrability inside the joint, with novices having to undergo a long training period [22] and experts often making mistakes with clinical consequences [26].

The reconstruction of the ACL illustrates well the aforementioned situation. The ACL rupture is a common medical condition with more than 200 000 annual cases in the USA alone [26]. The standard way of treatment is arthroscopic reconstruction where the torn ligament is replaced by a tissue graft that is pulled into the knee joint through tunnels opened with a drill in both femur and tibia [5]. Opening these tunnels in an anatomically correct position is crucial for knee stability and patient satisfaction, with the ideal graft being placed in the exact same position of the original ligament to maximize proprioception [2]. Unfortunately, ligament position varies significantly across individuals and, despite the substantial effort to model variance and provide anatomic references to be used during surgery [9], correct tunnel placement is still a matter of experience with success rates varying broadly between low and high volume surgeons [26]. Some studies reveal levels of patient satisfaction of only 75% with an incidence of revision surgeries of 10 to 15%, half of which caused by deficient technical execution [26]. Other studies show that even the most experienced surgeons fail in placing the graft in native position [11], which decreases patient satisfaction by reducing proprioception [2]. This is a scenario where Computer-Aided Surgery (CAS) can add substantial value by decreasing the learning curve of novice surgeons [1], preventing errors of clinical consequence, and enabling truly personalised ACL reconstruction.

Despite the clear clinical need, the solutions for Computer-Aided Arthroscopy (CAA) that have been proposed so far never met the expectations, and the use of navigation in ACL reconstruction is limited to a couple of research sites. One of the main problems is that current systems rely in optical-tracking that is simply too invasive to be used in arthroscopy. Thus, we propose a new approach to CAA where optical-tracking is replaced by video-tracking with all 3D measurements and inference being accomplished by processing the existing arthroscopic video in real-time.

1.1 Related work

The first solution for computer-aided ACL reconstruction was the Surgetics system from Praxim that dates back to the 90's [7]. The system employs a stereo infrared (IR) camera that tracks reflective markers attached to femur, tibia or instruments in order to estimate their 3D pose in real-time (optical-tracking). The solution relies in bone morphing where a tracked touch-probe is used to reference landmarks inside the joint to enable the system to build a 3D model from a known statistical 3D model of the knee and guide tunnel opening [23]. This image-free navigation approach was later followed by other companies such as B. Braun that still commercialises the Orthopilot system [1]. Since finding the bony landmarks tends to be time consuming and error prone, systems like the VectorVision from Brainlab replace bone morphing by fluoroscopy images acquired intra-operatively [5, 27]. This image-based navigation improves accuracy at the expense of using ionising radiation during the procedure that otherwise would not be required. To avoid this drawback, Cho *et al.* have recently proposed MRI-based navigation where the tunnel location is planned in a pre-operative MRI originally acquired for diagnosis, that is then registered with the patient's anatomy to guide surgical execution [6]. They reported results in tunnel placement in successive cadaver experiments with an average error of 2.9mm in footprint location and 7.13deg in tunnel orientation.

After 20 years since market inception of the first system [7], and despite many other alternatives advanced in the meanwhile [5, 1, 27, 6], the adoption of surgical navigation in arthroscopic ACL reconstruction is marginal because of its inaccuracy, inconvenience [13] and cost [19]. The optical-tracking technology has several drawbacks, such as bulky markers attached to instruments, preservation of lines-of-sight that disturbe surgical routine, and high-cost of equipment, that are well known in the context of navigated open surgery. Its use in arthroscopy has an additional major inconvenience that is invasiveness: the surgeon must open additional incisions to attach markers to the bone anatomy, which is a major obstacle for adoption because the objective of arthroscopy is exactly to minimize the number and size of incisions [29]. Conventional optical-tracking is not well suited for minimally invasive procedures and a system for navigated arthroscopy should ideally rely in processing the already existing intra-operative video. This solution would avoid the above mentioned inconveniences and promote cost efficiency by not requiring additional capital equipment.

Unfortunately, and despite the intense research in CAS using endoscopic video [18], arthroscopic sequences are specially challenging because of poor texture, existence of deformable tissues, complex illumination, and very close range acquisition. In addition, the camera is hand-held, the lens scope rotates, the procedure is performed in wet medium and the surgeon often switches camera portal. Our attempts of using visual SLAM pipelines, reported to work in laparoscopy [17], were unfruitful and revealed the need of additional visual aids to accomplish the robustness required for real clinical uptake.

1.2 Contributions and article overview

This article is an extension of the previous conference paper [25] and describes the first video-based system for CAA, where visual information is used to register a pre-operative CT/MRI with the patient anatomy such that tunnels can be opened in the position of the original ligament (patient specific surgery). The concept relates with previous works in CAS for laparoscopy that visually track a planar pattern engraved in a projector to determine its 3D pose [8]. We propose to attach similar fiducial markers to both anatomy and instruments in order to overcome the challenges in processing arthroscopic sequences. The marker attached to femur (or tibia) establishes a reference for the world coordinate system in which all the tracking is done. The moving arthroscope acts as a measuring device that visually estimates the relative 3D pose between markers such that instruments can be located in world coordinates (Fig. 1(a)). The scheme enables to perform accurate 3D reconstruction of points and curves in the bone surface using a tracked touch-probe (Fig. 1(b)). This 3D data is then fed into a specially designed registration algorithm [24] that overlays the pre-operative plan with the patient anatomy (Fig. 1(c)). Since all 3D data is stored in world coordinates, the guidance information is overlaid in the video whenever the femur (or tibia) marker is viewed by the camera (Fig. 1(d)).

The paper describes the proposed concept for video-based tracking (Section 2), overviews the surgical workflow for navigated ACL reconstruction (Section 3), and details the underlying image software pipeline including a performance evaluation of key modules that were carefully engineered to meet the application requirements (Section 4). The method is described with more detail than in [25], allowing a better understanding of the full pipeline, and the experimental evidence on the importance of the key modules is novel. Finally, Section 5 reports new experimental results in CAA for ACL reconstruction obtained both in phantom and in two cadaver labs. The tests in realistic *ex-vivo* conditions proved clinical feasibility and showed an accuracy in tunnel placement above what was reported in [6]. These are promising results that suggest that video-based CAA might be the solution for the broad adoption of computer navigation in arthroscopy.

2 Video-based computer-aided arthroscopy

This section overviews the proposed concept for CAA that uses the intra-operative arthroscopic video, together with planar visual markers attached to instruments and anatomy, to perform tracking and 3D pose estimation inside the articular joint. As discussed, applying conventional SLAM/SfM algorithms [17] to arthroscopic images is extremely challenging due to several issues such as the lack of texture, existence of shadows, highlights, fog and condensation, and the fact that we are working in a liquid medium at very close range. In order to circumvent such difficulties, we propose to use small planar fiducial markers that can be easily detected in images and whose pose

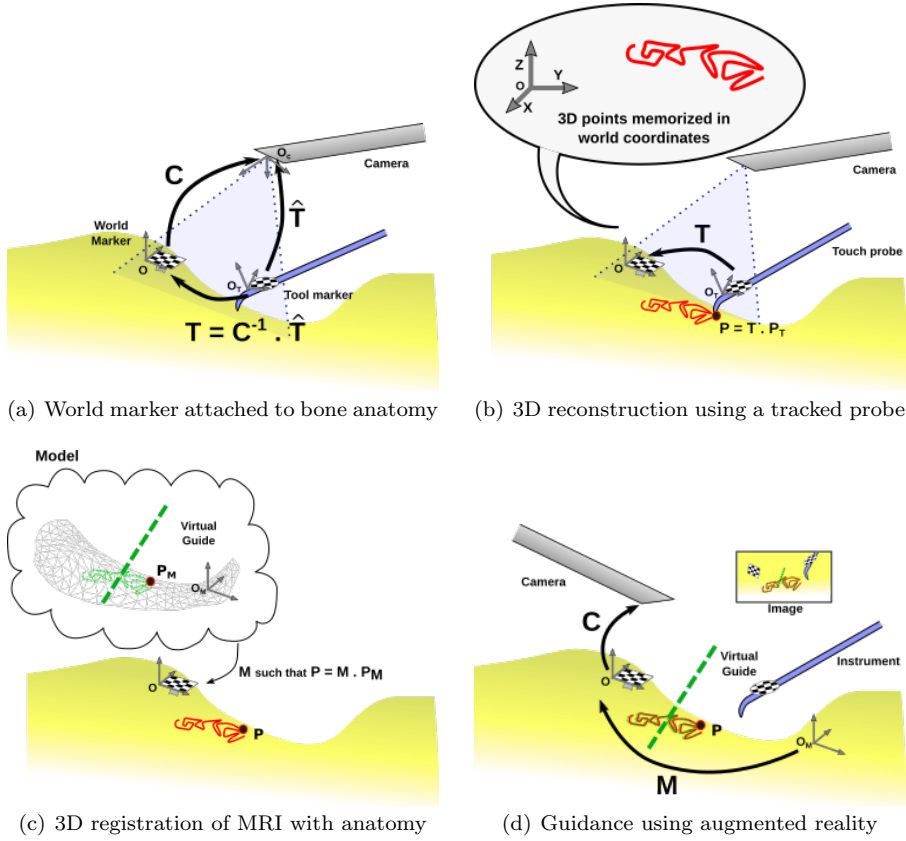


Fig. 1: Key steps of the proposed approach: (a) 3D pose estimation inside the articular joint, (b) 3D reconstruction of points and contours on bone surface, (c) 3D registration of a pre-operative model with the anatomy, and (d) guidance information overlaid in the arthroscopic video using augmented reality.

can be estimated using homography factorization [16,3]. These visual aids enable to achieve the robustness and accuracy required for deployment in real arthroscopic scenario that otherwise would be impossible. The key steps of the approach are the illustrated in Fig. 1 and described next.

The anatomy marker WM: The surgeon starts by rigidly attaching a screw-like object with a head of planar surfaces, each having an engraved known 4mm-side square pattern. We will refer to this screw as the World Marker (WM) because the local reference frame of its pattern will define the coordinate system with respect to which all 3D information is described. This is a very convenient feature in arthroscopy where the surgeon can have the camera in one portal, interrupt tracking to switch portals, and resume navigation as soon as the marker is detected again by the camera, without losing any of the previous markings or stored 3D info. The setup is illustrated in

Fig. 1(a). The WM can be placed in an arbitrary position in the intercondylar surface, as long as that it can be easily seen by the arthroscope during the procedure. The placement of the marker is accomplished using a custom made tool that can be seen in Fig. 3.

3D reconstruction of points and contours on bone surface: The 3D pose C of the WM in camera coordinates can be determined at each time instant by detecting the WM in the image, estimating the plane-to-image homography from the 4 detected corners of its pattern and decomposing the homography to obtain the rigid transformation [16,3]. Consider a touch probe that is also instrumented with another planar pattern that can be visually read. Using a similar method, it is possible to detect and identify the tool marker (TM) in the image and compute its 3D pose \hat{T} with respect to the camera. This allows the pose T of the TM in WM coordinates to be determined in a straightforward manner by $T = C^{-1}\hat{T}$ (Fig. 1(a)).

The location of the tip of the touch probe in the local TM reference frame is known, meaning that its location w.r.t. the WM can be determined using T . A point on the surface can be determined by touching it with the touch probe. A curve and/or sparse bone surface reconstruction can be accomplished in a similar manner by performing a random walk. Fig. 1(b) depicts this process, showing in red the reconstructed contour.

3D registration: The reconstructed contours and/or points are registered with the 3D pre-operative model, either by using point correspondences [12] or recent algorithms for curve-surface registration [24]. We will discuss in more detail how this registration is accomplished in a later section. As shown in Fig. 1(c), this registration will enable the pre-operative model to be overlaid in the bone surface, and thus all measurements and planning performed in the model, such as the tunnel position and orientation, can be transferred to the patient's anatomy.

Guidance using augmented and virtual realities: Since the proposed system relies solely in the arthroscopic video, augmented reality (AR) is a particularly natural way to provide guidance information. This is in line with the recent trend of mixed reality in surgery triggered by the developments in see-through displays [10]. However, virtual reality (VR) may also be advantageous in certain situations, and thus it is also employed during guidance. The tunnel can be opened in the planned position and orientation using a drill guide instrumented with a visual marker and whose symmetry axis's location is known in the marker's reference frame. This way, the location of the drill guide w.r.t. the pre-operative plan is known, providing real-time guidance to the surgeon, as illustrated in Fig. 1(d).

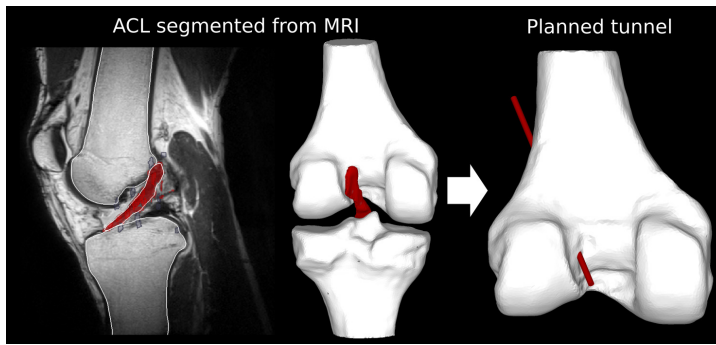


Fig. 2: The segmentation of the ACL using the pre-operative model allows the planning of the femoral tunnel to be performed according to the location of the native ligament, increasing proprioception.

3 Surgical workflow

3.1 Pre-operative steps

Typically, ACL reconstruction procedures require a pre-operative MRI of the knee to diagnose and/or confirm the existence of a torn ligament before proceeding to surgery. Our image-based approach makes use of this MRI not only in the registration and guidance steps described in Section 2, but also for segmenting the ACL, whenever possible, to be used as a reference to plan both the femoral and the tibial tunnels (Fig. 2). This allows the graft to be placed in the native ligament’s position, which is something that cannot be accomplished without computer guidance [11]. The advantages of such planning are twofold: first, it avoids technical mistakes that can lead to revisions surgeries, and secondly it improves patient satisfaction by maximising proprioception [2].

3.2 Intra-operative Steps

The steps of the complete surgical workflow are given in Fig. 3. An initial camera calibration using a single image of a checkerboard pattern is performed. Then, the world marker is rigidly attached to the anatomy and 3D points on the bone surface are reconstructed by touching it with an instrumented touch probe. While the points are being reconstructed and using the pre-operative model, the system performs an on-the-fly registration that will allow the drilling of the tunnel to be guided. Guidance information is given using augmented reality, by overlaying the pre-operative plan with the anatomy in real time, and using virtual reality, by continuously showing the location of the drill guide in the model reference frame. As a final step, the WM must be removed. Details are given below.

A: Since the camera has exchangeable optics, calibration must be made in the OR before starting the medical procedure. In addition, the lens scope

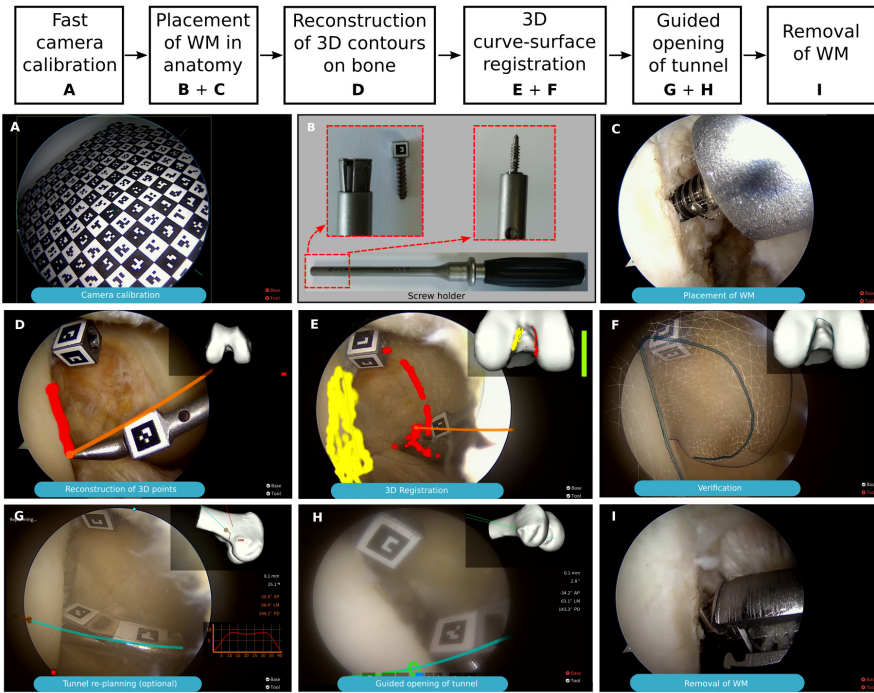


Fig. 3: Complete sequence of steps of the proposed CAA system.

rotates during the procedure, meaning that intrinsics must be adapted on the fly for greater accuracy. This is accomplished using an implementation of the method described in [21]. Calibration is done by collecting one image of a checkerboard pattern to determine intrinsics and radial distortion. Since the lens scope rotates, the center of rotation is determined on the fly by detecting the triangular mark and the boundary contour of the lens. For facilitating the process, acquisition is carried in dry environment and adaptation for wet is performed by multiplying the focal length by the ratio of the refractive indices [14]. This specifically designed calibration procedure conciliates robustness with minimum user effort.

B: In order to minimize the effort by the surgeon, the WM must be placed quickly and without the risk of falling. To accomplish this, we designed a grip-like tool - the screw holder - that grabs the cube-shaped head of the marker and retains it inside a hollow cylindrical body to make sure it does not fall. The marker is screwed in the desired location and afterwards the surgeon opens the screw holder to release the marker head.

C: The WM can be attached to any suitable location that provides good visibility by the arthroscope. From our experience, we consider that the best place is in the lateral wall of the intercondylar notch in the anterior and distal region. This area is easily reached and can be easily observed by the camera.

D: 3D points and contours are reconstructed by touching the bone surface with an instrumented probe. The regions that are typically accessible and digitized for registration are the posterior region in the lateral wall and the anterior region in the medial wall of the intercondylar notch.

E: As soon as the bone surface starts being reconstructed, an on-the-fly registration algorithm begins, with registration attempts being performed successively. While this process occurs, a progress bar indicating the evolution of the registration results is available. Simultaneously, it is possible to observe the reconstructed points being fitted to the 3D model in VR, providing another indication of the progress of the registration.

F: After registration is finished, it is crucial that the surgeon has some kind of verification method that provides assurance that the obtained registration is accurate. For this, we use AR to overlay different highlights on the patient's anatomy, such as the blumensaat's line and the contour of the intercondylar region.

G: There are times when it is impossible to drill the bone tunnel as initially planned as it is inaccessible from the opened surgical portals. To account for this, our system enables the surgeon to intra-operatively adjust the orientation of the tunnel in real time, allowing also the anticipation of the location of the exit point with high accuracy.

H: The drilling of the tunnel is guided using AR to overlay in the image both the position and orientation of the planned tunnel and the orientation of the guide tool in real-time. When both are aligned, the planned tunnel turns green and the drilling can be done.

I: As a final step, the WM is safely removed by making use of the screw holder for grabbing its head and unscrewing it.

This paper does not provide details on the placement of the tibial tunnel because the procedure is similar to the one described here for the placement of the femoral tunnel. The accompanying video shows the procedure being performed on both femur and tibia.

4 Key software modules

This section provides details on three key modules of the system, namely the camera calibration, the marker pose estimation and the registration stages. Each module's performance is tested and the relevance of the proposed improvements is demonstrated.

4.1 Camera modeling and calibration

The first step of the pipeline is the calibration of the arthroscopic camera for finding its intrinsics and radial distortion that will allow correct 3D measurements on the anatomy to be performed. Our system employs the method

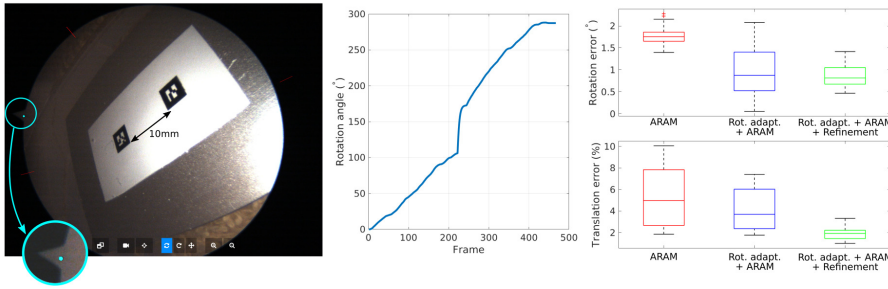


Fig. 4: Experiment on lens rotation in wet environment. A video sequence showing two markers with known relative pose is acquired while rotating the lens scope. For each frame, the rotation and translation errors w.r.t. the ground truth are computed and their distributions are shown in the boxplots on the right.

presented in [21] for this task, with the camera being calibrated with a single image of a checkerboard pattern before the medical procedure. Since the lens scope rotates and it is not feasible to calibrate the arthroscope for every possible lens position, the calibration parameters are updated on-the-fly as explained in [21]. During the procedure, the triangular mark and the boundary contour are detected in each frame i , providing the lens rotation w.r.t. the calibration image. This 2D rotation is parameterized by the angle α_i and the fixed point \mathbf{q}_i that serve as input for updating the matrix of intrinsic parameters \mathbf{K}_i . Since the radial distortion is a characteristic of the lens, the parameter ξ , which quantifies the amount of radial distortion, is unaffected by the relative motion of the lens with respect to the camera-head.

For each frame i , the matrix of intrinsic parameters \mathbf{K}_i becomes

$$\mathbf{K}_i \sim \mathbf{R}_{\alpha_i, \mathbf{q}_i} \mathbf{K}_0, \quad (1)$$

with \sim denoting equality up to scale, \mathbf{K}_0 being the matrix of intrinsic parameters obtained in the single image calibration and $\mathbf{R}_{\alpha_i, \mathbf{q}_i}$ being the 2D rotation of α_i radians around the point \mathbf{q}_i .

In order to assess the influence of adapting the camera intrinsics according to the lens rotation, we performed an experiment where we calibrated the camera using a single checkerboard image and then acquired a 500-frame video sequence of a ruler with two 2.89mm-side square markers 10mm apart in wet environment. The rotation of the scope performed during the acquisition of the video is quantified in the plot in the middle of Fig. 4 that shows that the total amount of rotation was almost 300°. The lens mark, shown in greater detail in Fig. 4, is detected in each frame for compensating the intrinsics.

The accuracy of the method is evaluated by computing the relative pose between the two markers in each frame and comparing it with the ground truth pose. The relative pose is computed both with and without rotation adaptation and the distribution of errors are given in the red and blue boxplots,

respectively. Details on how each marker’s pose is computed are given in the next section.

Results clearly show that adapting for the lens rotation is crucial to have high accuracy in marker pose estimation. In more detail, it significantly improves the pose estimation in terms of rotation, with median errors dropping about 1° . Concerning the translation, the median error decreases nearly 2 percentage points, and the error distribution is narrower, meaning that the estimated translations are more coherent for different lens positions.

4.2 Pose estimation of fiducial markers

There are several publicly available libraries for augmented reality that implement the process of detection, identification and pose estimation of square markers. We opted for the ARAM library [3] that, in general terms, starts by detecting squares in images using edge detection, line fitting and corner estimation. Then, squares that do not contain a marker are discarded and the remaining ones go through an identification stage. The four corners of each identified marker are used for estimating a planar homography, whose decomposition provides the pose of the marker with respect to the camera.

This standard procedure does not reach the accuracy levels required by our system. Thus, we complemented it with an optimization stage that uses photoconsistency to refine the marker pose. This is done as described in [20] with the extension to accommodate radial distortion as in [15]. For each marker, we also determine the median black and white intensity values and use that information to compensate for illumination changes.

The effect of the new photogeometry refinement stage is evaluated by including it in the estimation of the pose of the markers in the previous experiment. The distributions of rotation and translation errors are shown as green boxplots in Fig. 4, making it evident that this additional stage is indispensable for good accuracy. Errors decrease substantially, reaching median values as low as 0.8° and 1.7%.

4.3 Registration

Registration is accomplished with the method presented in [24] for curve-surface registration. It is a method for global registration that does not require the surgeon to pinpoint landmarks since it automatically finds pairs of matching points in the curve and in the surface, along with their tangents and normals, for estimating the rigid transformation between the pre-operative model and the patient’s anatomy. Let \mathbf{P}, \mathbf{Q} with tangents \mathbf{p}, \mathbf{q} be a pair of points from the curve (Fig. 5). The algorithm finds all matching pairs of points $\hat{\mathbf{P}}, \hat{\mathbf{Q}}$ with normals $\hat{\mathbf{p}}, \hat{\mathbf{q}}$ on the surface using a set of conditions that depend on the differential information (tangents and normals). Then, an hypothesis-and-test

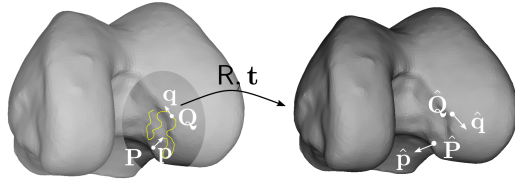


Fig. 5: The rigid transformation R, t is determined by searching for pairs of points P, Q with tangents p, q on the curve side that are a match with pairs of points \hat{P}, \hat{Q} with normals \hat{p}, \hat{q} on the surface side.

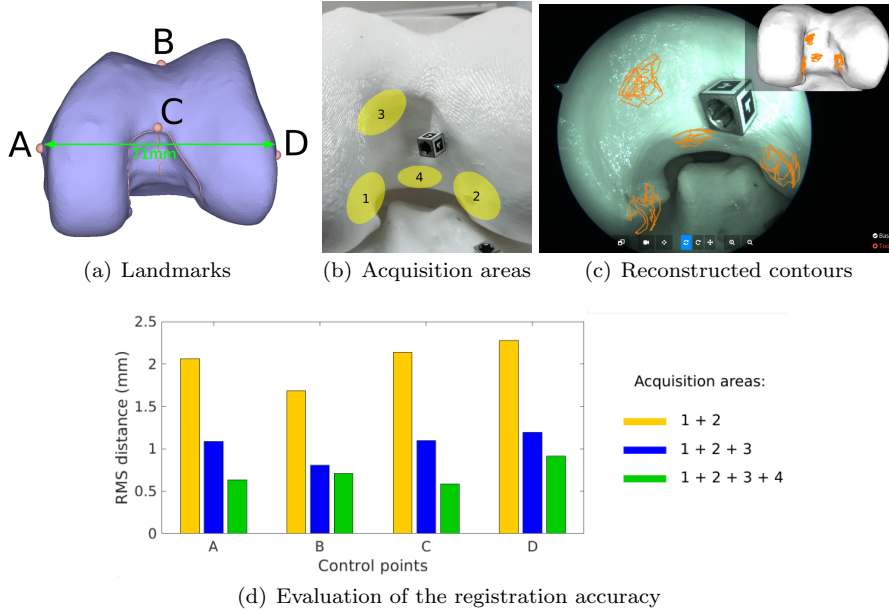


Fig. 6: Analysis of performance of the registration algorithm with different levels of spreading of reconstructed bone surface.

framework finds the rigid transformation that best aligns the reconstructed curve with the pre-operative surface. A final standard ICP step [4] is performed for refining the solution.

In the ACL reconstruction procedure, the surgeon only has access to the intercondylar region, making the area of reconstructed points and contours to be limited. Since this may have an impact on registration accuracy, we performed an experiment where we successively increase the area of reconstructed bone surface and use 4 control points to provide a metric of accuracy.

Fig. 6(a) shows the 4 control points chosen for assessing the registration accuracy, which are located very far from the area considered for registration (the intercondylar region). This test was performed on a dry model and

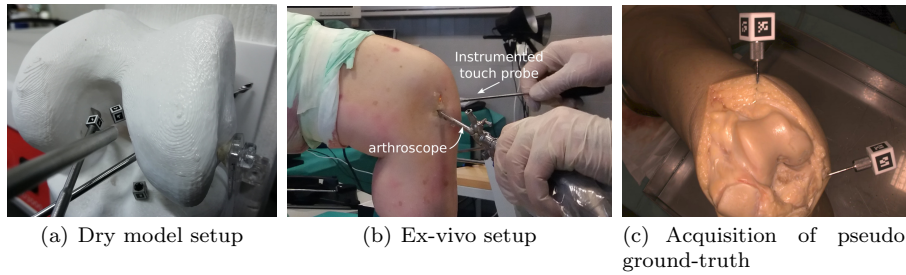


Fig. 7: Analysis of performance of the registration algorithm in two kinds experiments: one in the laboratory using a dry knee model and another using *ex-vivo* data.

consisted in reconstructing 10 different sets of curves by scratching the bone surface on the acquisition areas depicted in Fig. 6(b) with an instrumented touch probe, and registering them with the virtual model shown in Fig. 6(a). Fig. 6(c) shows an image of the reconstructed contours overlaid on the dry model. This test was performed incrementally, by first registering only with contours acquired in areas 1 and 2, then also with area 3 and finally with area 4.

Using each solution, the 4 control points are transformed to the WM reference frame and their centroids are computed. Then, the RMS distance between each transformed point and the corresponding centroid is determined and shown in Fig. 6(d), providing a quantitative assessment of the registration accuracy. Results show that although RMS errors of only about 2 mm are obtained with the smallest spread, increasing it leads to better results, which is expected since it decreases the ambiguity in the solution. For the largest spread, all RMS distances are below 0.9mm, despite the control points belonging to regions that are very distant from the reconstructed area.

5 Experiments

This section reports experiments that assess the performance of the registration of a pre-operative model with the patient's anatomy. Tests on laboratory and using *ex-vivo* data are performed. Whenever possible, the accuracy of the opened femoral tunnel is also assessed.

All experiments were performed in a PC that is connected in-between camera tower and display. The PC is equipped with a frame grabber Datapath Limited DGC167 in an Intel Core i7 4790 and a GPU NVIDIA GeForce GTX950 that was able to run the pipeline in HD format at 60fps with latency of 3 frames. In addition, we built all the markers, custom screw holder tool, touch probe and drill guide that can be seen in Fig. 3 and in the accompanying video.

Table 1: RMS distances for the 4 control points in mm.

	Dry model	Ex-vivo 1	Ex-vivo 2
A	0.85	1.82	1.56
B	0.63	1.23	1.73
C	0.82	1.46	1.71
D	0.77	1.02	1.05
# trials	10	4	4

Table 2: Distances measured in the footprint (mm).

Trial	Our approach		Results from [6]
	Dry model	Ex-vivo 2	
1	0.44	2.54	-
2	0.35	2.55	4.21
3	0.39	2.54	3.04
4	0.38	2.98	1.47
RMS	0.39	2.66	3.12

Table 3: Angles between the vectors of the planned and the created tunnels (deg).

Trial	Our approach		Results from [6]
	Dry model	Ex-vivo 2	
1	0.34	3.71	-
2	0.39	4.13	6.97
3	0.27	1.87	7.92
4	0.15	1.84	6.5
RMS	0.30	3.07	7.15

5.1 Experiments on dry model

A dry knee model 3D printed with the planned tunnel (Fig. 7(a)), which we consider as ground truth since the accuracy of 3D printing is high, was used for acquiring 10 trajectories with unconstrained motion, which were registered with the corresponding virtual model. Similarly to the experiment described in Section 4.3, we considered 4 control points and computed their RMS distances, which are shown in Table 1. Errors below 1mm are obtained for all control points, confirming that the registration algorithm is able to achieve high accuracy. Also, using unrestricted contours leads to similar results as with the 4 acquisition areas in the previous experiment, which indicates that having contours reconstructed only on these areas is sufficient for obtaining high-quality registrations.

In 4 random registration attempts, we inserted an instrumented tool in the tunnel and measured its orientation and the location of the footprint in WM coordinates. Then, using the corresponding registration result, we transformed these measurements into the virtual model reference frame and computed the distance to the ground truth footprint and the angle between the measured and the ground truth orientations. Results are given in Tables 2 and 3, respectively, demonstrating that the measured and opened tunnels are very similar, with errors below half a millimeter in the footprint and 0.4° in orientation.

5.2 *Ex-vivo* experiments

Two experiments were performed on *ex-vivo* data, and followed a similar strategy as the one on the dry model, having the difference that the total number of registration attempts was 4 for each cadaver specimen. Fig. 7(b) illustrates the setup of the *ex-vivo* experiment and Table 1 gives the quantitative analysis of the obtained registration results. A slight degradation in accuracy w.r.t. the dry model test is observed, which is expected since the latter is a more controlled environment. However, the obtained accuracy is very satisfactory, with the RMS distances of all control points being below 2mm.

Concerning the second *ex-vivo* experiment, we also performed the measurement of the opened tunnel as in the dry model experiment. Since there was only one cadaver specimen available, we opened the tunnel in trial 1 and measured that same tunnel in the remaining registration attempts using the instrumented guide tool. In this case, to have pseudo ground truth information of the location of the footprint and the orientation of the tunnel, after the procedure the knee was opened (Fig. 7(c)) and we used optical tracking for reconstructing the opened tunnel. This was done by inserting a k-wire into the tunnel and reconstructing 3D points on its surface by touching it with an instrumented probe, which were then fitted to a line. The femur was also carefully registered with the pre-operative model in order to transform these measurements into the model's reference frame. Tables 2 and 3 show the errors obtained in our *ex-vivo* experiment as well as the errors reported in [6], which were obtained using 4 cadaveric knees. Since in [6] it is reported that accuracy increased as the experiment proceeded, and the execution with the first cadaveric knee yielded a result that was clearly an outlier, we do not include it, for the sake of fairness. Our method provides higher accuracy than [6] in all but one trial in the footprint's location, being substantially superior in terms of orientation of the opened tunnel for all cases.

In all trials of both *ex-vivo* experiments, the attachment and removal of the WM took less than 2 minutes, and the surgeons considered it an easy and safe process that does not add significant overhead to the medical procedure.

This experiment demonstrates that our proposed system is very accurate in aligning the anatomy with a pre-operative model of the bone, enabling a reliable guidance of the ACL reconstruction procedure.

6 Conclusions

This paper presents the first video-based navigation system for ACL reconstruction. The software is able to handle unconstrained lens rotation and register pre-operative 3D models with the patient's anatomy with high accuracy, as demonstrated by the experiments performed both on phantom and using *ex-vivo* data. In addition, the cadaver lab also demonstrated that the approach is clinically feasible with the marker being placed and removed very quickly without the risk of falling and becoming a lost free body inside the joint.

The results are clearly encouraging: the high accuracy and short time overhead combined with no additional incisions or capital equipment make this video-based CAA solution an appealing proposition. As future work, we will investigate ways of measuring ligament balancing inside the joint as well as target other procedures that might benefit from navigation such as the resection of Femuro Acetabular Impingement during hip arthroscopy.

Compliance with ethical standards

Conflict of interest

The authors declare that they have no conflict of interest.

Ethical approval

All studies involving post-mortem subjects followed the procedures for informed consent that are described in the Declaration of Helsinki.

Informed consent

Informed consent was obtained from all individual participants included in the study.

References

1. Anthony, C.A., Duchman, K., McCunniff, P., McDermott, S., Bollier, M., Thedens, D.R., Wolf, B.R., Albright, J.P.: Double-bundle acl reconstruction: Novice surgeons utilizing computer-assisted navigation versus experienced surgeons. In: *Computer Aided Surgery* (2013)
2. Barrett, D.S.: Proprioception and function after anterior cruciate reconstruction. In: *J Bone Joint Surg Br* (1991)
3. Belhaoua, A., Kornmann, A., Radoux, J.: Accuracy analysis of an augmented reality system. In: *ICSP* (2014)
4. Besl, P.J., McKay, N.D.: A method for registration of 3-d shapes. *IEEE Transactions on Pattern Analysis and Machine Intelligence* (1992)
5. Brown, C.H., Spalding, T., Robb, C.: Medial portal technique for single-bundle anatomical anterior cruciate ligament (acl) reconstruction. In: *Int Orthop* (2013)
6. Cho, W.J., Kim, J.M., Kim, D.E., Lee, J.G., Park, J.W., Han, Y.H., Seo, H.G.: Accuracy of the femoral tunnel position in robot-assisted anterior cruciate ligament reconstruction using a magnetic resonance imaging-based navigation system: A preliminary report. In: *The International Journal of Medical Robotics and Computer Assisted Surgery* (2018)
7. Dessenne, V., Lavallée, S., Julliard, R., Orti, R., Martelli, S., Cinquin, P.: Computer-assisted knee anterior cruciate ligament reconstruction: First clinical tests. In: *Journal of Image Guided Surgery* (1995)
8. Edgcombe, P., Pratt, P., Yang, G.Z., Nguan, C., Rohling, R.: Pico lantern: A pick-up projector for augmented reality in laparoscopic surgery. In: *MICCAI* (2014)

9. Forsythe, B., Kopf, S., Wong, A.K., Martins, C.A.Q., Anderst, W., Tashman, S., Fu, F.H.: The location of femoral and tibial tunnels in anatomic double-bundle anterior cruciate ligament reconstruction analyzed by three-dimensional computed tomography models. In: *J Bone Joint Surg Am* (2010)
10. Hajek, J., Unberath, M., Fotouhi, J., Bier, B., Lee, S.C., Osgood, G., Maier, A., Armand, M., Navab, N.: Closing the calibration loop: An inside-out-tracking paradigm for augmented reality in orthopedic surgery. In: *21st International Conference on Medical Image Computing and Computer Assisted Intervention, MICCAI 2018* (2018)
11. Hart, A., Sivakumaran, T., Burman, M., Powell, T., Martineau, P.A.: A prospective evaluation of femoral tunnel placement for anatomic anterior cruciate ligament reconstruction using 3-dimensional magnetic resonance imaging. In: *The American Journal of Sports Medicine* (2017)
12. Horn, B.K.P.: Closed-form solution of absolute orientation using unit quaternions. *Journal of the Optical Society of America A* (1987)
13. Kim, Y., Lee, B.H., Mekuria, K., Cho, H., Park, S., Wang, J.H., Lee, D.: Registration accuracy enhancement of a surgical navigation system for anterior cruciate ligament reconstruction: A phantom and cadaveric study. In: *The Knee* (2017)
14. Lavest, J.M., Rives, G., Lapreste, J.T.: Dry camera calibration for underwater applications. In: *MVA* (2003)
15. Lourenço, M., Barreto, J.P., Fonseca, F., Ferreira, H., Duarte, R.M., Correia-Pinto, J.: Continuous zoom calibration by tracking salient points in endoscopic video. In: *MICCAI* (2014)
16. Ma, Y., Soatto, S., Kosecka, J., Sastry, S.: An invitation to 3-d vision: from images to geometric models. In: *Springer* (2004)
17. Mahmoud, N., Cirauqui, I., Hostettler, A., Doignon, C., Soler, L., Marescaux, J., Montiel, J.M.M.: Orbslam-based endoscope tracking and 3d reconstruction. In: *CARE@MICCAI* (2016)
18. Maier-Hein, L., Mountney, P., Bartoli, A., Elhawary, H., Elson, D., Groch, A., Kolb, A., Rodrigues, M., Sorger, J., Speidel, S., Stoyanov, D.: Optical techniques for 3d surface reconstruction in computer-assisted laparoscopic surgery. In: *Medical image analysis* (2013)
19. Margier, J., Tchouda, S.D., Banihachemi, J.J., Bosson, J.L., Plaweski, S.: Computer-assisted navigation in acl reconstruction is attractive but not yet cost efficient. In: *Knee Surg Sports Traumatol Arthrosc* (2014)
20. Mei, C., Benhimane, S., Malis, E., Rives, P.: Efficient homography-based tracking and 3-d reconstruction for single-viewpoint sensors. In: *T-RO* (2008)
21. Melo, R., Barreto, J.P., Falcao, G.: A new solution for camera calibration and real-time image distortion correction in medical endoscopy - initial technical evaluation. In: *TBE* (2012)
22. Nawabi, D.H., Mehta, N.: Learning curve for hip arthroscopy steeper than expected. In: *J Hip Preserv Surg* (2000)
23. Plaweski, S., Pearle, A., Granchi, C., Julliard, R.: Praxim acl navigation system using bone morphing. In: *Navigation and MIS in Orthopedic Surgery* (2007)
24. Raposo, C., Barreto, J.P.: 3d registration of curves and surfaces using local differential information. In: *CVPR* (2018)
25. Raposo, C., Sousa, C., Ribeiro, L.L., Melo, R., Barreto, J.P., Oliveira, J., Marques, P., Fonseca, F.: Video-based computer aided arthroscopy for patient specific reconstruction of the anterior cruciate ligament. In: *MICCAI* (2018)
26. Samitier, G., Marcato, A.I., Alentorn-Geli, E., Cugat, R., Farmer, K.W., Moser, M.W.: Failure of anterior cruciate ligament reconstruction. In: *ABJS* (2015)
27. Shafizadeh, S., Paffrath, T., S. Grote, J.H., Tiling, T., Bouillon, B.: Fluoroscopic-based acl navigation. In: *Navigation and MIS in Orthopedic Surgery* (2007)
28. Treuting, R.: Minimally invasive orthopedic surgery: arthroscopy. In: *The Ochsner Journal* (2000)
29. Zaffagnini, S., Klos, T.V., Bignozzi, S.: Computer-assisted anterior cruciate ligament reconstruction: An evidence-based approach of the first 15 years. In: *Arthroscopy: The Journal of Arthroscopic and Related Surgery* (2010)